



# Design and development of novel Co-MOF nanostructures as an excellent catalyst for alcohol oxidation and Henry reaction, with a potential antibacterial activity

Sima Aryanejad<sup>1</sup> | Ghodsieh Bagherzade<sup>1</sup> | Maryam Moudi<sup>2</sup>

<sup>1</sup>Department of Chemistry, Faculty of Sciences, University of Birjand, Birjand, 97175-615, Iran

<sup>2</sup>Department of Biology, Faculty of Sciences, University of Birjand, Birjand, 97175-615, Iran

## Correspondence

Ghodsieh Bagherzade, Department of Chemistry, Faculty of Sciences, University of Birjand, Birjand, 97175-615, Iran.  
Email: bagherzadeh@birjand.ac.ir;  
gbagherzade@gmail.com

## Funding information

University of Birjand Research Council; Iran National Science Foundation, Grant/Award Number: 96008530

The novel metal–organic framework  $\text{Co}_2(\text{bdda})_{1.5}(\text{OAc})_1 \cdot 5\text{H}_2\text{O}$  (UoB-3) was synthesized via a simple method at room temperature. UoB-3 was characterized by the different methods, including X-ray diffraction (XRD), transmission electron microscopy (TEM), thermogravimetric analysis (TGA), Fourier transform infrared spectroscopy (FT-IR),  $\text{N}_2$ -adsorption/desorption and elemental analysis. The catalytic ability of UoB-3 was detected to be excellent for primary and secondary alcohols oxidation reaction with high yields under solvent-free conditions. Moreover, UoB-3 was highly active for Henry reaction of different aldehydes with nitromethane in water as a green solvent. The nanocatalyst can be recycled for five consecutive cycles without losing its activity and structural rigidity. The antibacterial activity of UoB-3 nanostructures towards Gram-negative bacteria, *Escherichia coli* and Gram-positive bacteria, *Bacillus cereus* was also evaluated by using an inhibition zone test. These nanostructures exhibited strong antibacterial effect against both of them. The purpose of this study was the developing metal–organic framework materials with the enhanced activity in various fields.

## KEYWORDS

alcohol oxidation, antibacterial activity, Henry reaction, MOF, Schiff base

## 1 | INTRODUCTION

The green chemistry revolution has provided a large number of challenges in practical and industrial chemistry fields. Some of the challenges for chemist include the finding and developing of new synthetic pathways by using alternative feedstocks and more selective. In addition, overcoming to these problems can be possible by changing reaction conditions and solvents for increasing selectivity, minimizing energy, designing less toxic and intrinsically safer chemicals.<sup>[1]</sup> A chemical synthesis will be ideal by a combination of a number of environmental, health, safety and economic purposes.<sup>[2–8]</sup> Metal–organic frameworks (MOFs) are one of chemical

compound that can be provided some of the green chemistry goals. In the last years, the researchers have observed the unprecedented explosion of a new class of porous metal–organic frameworks (MOFs).<sup>[9,10]</sup> The combination of organic and inorganic building blocks into highly ordered, crystalline structures offers an almost infinite number of compositions, enormous flexibility in pore size, shape, structure, and plenty opportunities for functionalization, grafting and encapsulation.<sup>[11]</sup> Because of these properties, MOFs have the numerous potential application in the areas of gas storage,<sup>[12]</sup> sensing,<sup>[13]</sup> separations,<sup>[14]</sup> catalysis,<sup>[15,16]</sup> drug delivery<sup>[17]</sup> and health science.<sup>[18]</sup> In spite of the many reported catalytic applications of MOFs, there is a challenge to develop truly

efficient and selective catalytic processes using MOFs. On the other hand, ability to access monodisperse nano-sized MOFs is very important for prospective applications in heterogeneous catalysis and biomedicine.<sup>[19,20]</sup>

Among the synthetic methods of aldehyde and ketones, the alcohol oxidation is very interesting in modern organic chemistry.<sup>[21–24]</sup> Hence, the development of alcohol oxidation methods directs toward achieving highly selective, efficient, and environmentally friendly catalytic systems. Also, it is important that the stoichiometric amount of inorganic oxidant is being substituted with green oxidant such as O<sub>2</sub> or peroxides or peroxides [H<sub>2</sub>O<sub>2</sub>, tert-butyl hydroperoxide (TBHP)] to overcome the formation of harmful wastes.<sup>[25,26]</sup> There are some reports on MOFs which are catalytically active for the alcohol oxidation reaction.<sup>[27–33]</sup> Despite of available reports, the search for new, environmentally friendly, and efficient alcohol oxidation protocols, as well as the improvement of the known ones, is of current interest.

On the other hand, the one of important methods for C-C formation is the nitro aldol or Henry reaction in modern organic chemistry.<sup>[34,35]</sup> The product of Henry reaction,  $\beta$ -nitroalkanols, could be readily transformed into beneficial synthons for the development of various natural products and pharmaceutically urgent structural scaffolds.<sup>[36,37]</sup> Additionally, the oxidation, dehydration, reduction and Nef reaction of  $\beta$ -nitroalkanols lead to a diverse of significant building blocks. These building blocks have many applications in synthetic chemistry for the complex molecules construction.<sup>[38–40]</sup> Therefore, for developing of the Henry reaction have made considerable efforts using homogeneous<sup>[41–43]</sup> and heterogeneous<sup>[44–47]</sup> catalysts. Among the studies have reported for heterogeneous-catalyzed Henry reaction until now, few reports exist about MOFs that catalyse this reaction.<sup>[48–50]</sup> It is not common that the metal catalysts act effective in environmentally water solvent.<sup>[51,52]</sup> Therefore, the replacing an organic solvent with this green solvent in both synthesis and catalysis has achieved advantages not only in the laboratory scale but also in the industrial scale.<sup>[53]</sup>

With respect to significance of the green chemistry goals and the potential application of MOFs, also our interest to this field, we focused on the synthesis and properties of MOFs in catalytic and antibacterial areas.

In our continuing research on synthesis and applications of MOFs,<sup>[54,55]</sup> we synthesized the new Co-MOF nanostructures from coordination assembly of cobalt acetate with 4,4'-[benzene-1,4-diylbis (methylidene-nitrilo)] dibenzoic acid (H<sub>2</sub>bdda) in water under ultrasound irradiation (viewed as UoB-3).

Hereby, we investigated the potential catalytic activity in primary/secondary alcohol oxidation under solvent-

free condition and Henry reaction in water as a green solvent. The results exhibited that UoB-3 would be a heterogeneous catalyst with highly efficiency and stable performance. The nano-catalyst can be easily recovered and reused due to its heterogeneous catalytic nature. In the following study of MOF applications, we have sought to use UoB-3 nanostructures as antibacterial agent. The evaluation of test towards both Gram-negative bacteria and Gram-positive bacteria revealed good potency for the bactericidal activity.

## 2 | EXPERIMENTAL

### 2.1 | Materials and instruments

All of the reagents and solvents employed were from the commercial sources and were used without further purification. TEM investigations were performed using a Philips CM120 Transmission Electron Microscope. XRD was conducted on a X'Pert Pro MPD diffractometer with Cu-K $\alpha$  ( $\lambda = 1.54060 \text{ \AA}$ ) radiation source. The Brunauer–Emmett–Teller (BET) surface area and pore sizes of the UoB-3 were measured using from N<sub>2</sub> adsorption/desorption isotherms at 77 K with a Belsorp mini II instrument after degassing UoB-3. The FT-IR spectra were recorded on a NICOLET system 800 beam splitter KBr SCAL = 800 using a resolution in the range of 400–4000 cm<sup>-1</sup>. The C, H, and N contents were determined using a Perkin Elmer CHNS-O Elemental Analyzer. Inductively coupled plasma atomic emission spectroscopy (ICP-AES) analysis was conducted on OPTIMA 7300DV. Thermoanalyzer Shimadzu was used for thermogravimetric analysis (TGA) between 30 and 710 °C with a heating rate of 10 °C/min under a N<sub>2</sub> flow. Ultrasonic generation was performed in an ultrasonic bath Bandelin electronic (frequency: 35 KHz). The reaction progress and product purity were released by TLC on silica gel polygram SILG/UV254 plates. NMR experiments were performed on a Bruker UltraShield™ spectrometer operating for proton-1 and carbon-13, respectively. The chemical shifts were expressed in ppm relative to tetramethylsilane as the internal reference.

### 2.2 | Synthesis of 4,4'-[benzene-1,4-diylbis (methylidene-nitrilo)] dibenzoic acid (H<sub>2</sub>bdda)

4-amino benzoic acid (2 mmol, 137 mg) was dissolved in EtOH (10 ml) and added gradually to a solution of terephthalaldehyde (1 mmol, 268 mg) in EtOH (5 ml). The mixture was magnetically stirred for one hour at the room temperature. After completion of the reaction,

the resulting yellow crystalline solid was filtered, washed with EtOH three times and then dried in the oven under vacuum.<sup>[55]</sup>

### 2.3 | Synthesis of nanoscaled co-MOF (UoB-3)

The Co-MOF nanostructures were synthesized according to a facile one-pot procedure. First, the linker H<sub>2</sub>bdda (0.372 g, 1 mmol) were dissolved by adding NaOH 10% (1 ml) in deionized water (20 ml) under magnetic stirring for 5 mins at room temperature to obtain a clear yellow solution. Then, a solution of Co (OAc)<sub>2</sub> (0.342 g, 2 mmol) in deionized water (10 ml) was added dropwise to above mixture under ultrasonic irradiation at room temperature for 15 mins and stay in the same condition for 30 mins. The resulting green precipitation was collected by centrifugation and washed with EtOH three times by dispersion. The resulting Co<sub>2</sub>(bdda)<sub>1.5</sub>(OAc)<sub>1</sub>·5H<sub>2</sub>O were dried in an oven at 100 °C. Elemental analysis and ICP (calc.%): C (49.91%), N (4.85%), H (3.98%) and Co (15.25%); (exp.%): C (50.43%), N (5.00%), H (3.56%) and Co (13.68%).

### 2.4 | Typical catalytic procedure for alcohol oxidation

Typically, a mixture of UoB-3 (2 mol%) as catalyst, alcohol (1 mmol) and TBHP (1.5 mmol) was stirred at 65 °C for appropriate time. The progress of the reaction was determined by thin layer chromatography (TLC). After completion, the reaction mixture was cooled to room temperature. The catalyst was separated by centrifugation, thoroughly washed with EtOAc and after drying, used in the next run. The products were purified on a silica gel plate to give pure products. For identification of the final products, their physical data were compared with those of authentic samples, because of all of them are known.

### 2.5 | Typical catalytic procedure for Henry reaction

In a typical experiment, aldehyde (1.0 mmol), nitromethane (5.0 mmol) and UoB-3 (3 mol%) were added to water (1 ml) in a glass vessel. Afterwards, the capped reaction system was stirred for 24 hrs at 70 °C. The solid catalyst was removed by centrifugation from the reaction mixture and the organic phase was extracted with CH<sub>2</sub>Cl<sub>2</sub> and dehydrated with Na<sub>2</sub>SO<sub>4</sub> to determine the conversion. After the evaporation of the solvent, the crude products

were purified on a silica gel plate (petroleum ether/ethyl acetate; 5:1) that were characterized with <sup>1</sup>HNMR. In addition, the recycling experiments were carried out after washing and drying the used catalyst. The rest of the process was followed as the same condition.

### 2.6 | Anti-bacterial activity

*Staphylococcus aureus* (Gram-positive) and *Escherichia coli* (Gram-negative) as the model microorganisms were used to assess the antibacterial activity of UoB-3 nanostructures. Experiments were performed with fresh bacteria previously incubated on Nutrient Agar plates at 37 °C for 24 hours. Agar plates were provided by dissolving agar powder (15.0 g L<sup>-1</sup>), tryptone (5.0 g L<sup>-1</sup>), yeast extract (2.5 g L<sup>-1</sup>), glucose (1.0 g L<sup>-1</sup>) in deionized water. The above mixture was heated and stirred until the agar dissolved. In the following, the pH of solution was adjusted to 7.0 ± 0.1 with sodium hydroxide or hydrochloric acid and the plates were sterilized by autoclaving.

The biocidal effect of UoB-3 was investigated by means of the diffusion method (Bauer et al., 1966). Therefore, the bacterial suspension (200 ml, containing 5·10<sup>7</sup> colony-forming units (CFU)/ml) was spread on the prepared agar plates. After drying plates, the holes (7 mm diameter) were punched by using the sterile tip over the agar plates. Then, UoB-3 (1 mg) was disposed directly onto the holes of agar plates, after which the plates were incubated at 37 °C for 48 hrs. The antibacterial activity was evaluated based on the standard zone of inhibition test. A qualitative test was performed under static conditions that the diameters of the growth inhibition zones were measured with the scale and reported in centimeter. The experiments were performed in two replicates.

## 3 | RESULT AND DISCUSSION

### 3.1 | Syntheses and characterization

The synthesis of UoB-3 nanostructures was performed under ultrasound irradiation conditions, by reacting the H<sub>2</sub>bdda with Co (OAc)<sub>2</sub> in the presence of deionized water at room temperature (Scheme 1).

TEM technique was used to get a further insight into the structure of UOB-3 nanostructures. Monodispersed nanoparticles with relatively uniform morphology were detected (Figure 1a). The average diameter of nanostructures was obtained 32 nm based on the particle size distribution histogram (Figure 1b).

Many efforts were made to gain the appropriate crystals for single-crystal structure determination. Unfortunately, the crystal size was very small which be



**SCHEME 1** Synthesis of UoB-3 nanostructures from Schiff base as organic linker

unsuitable for X-ray diffraction. However, the PXRD pattern of UoB-3 was used to investigate the structural properties (Figure 1c). It was clear that the most prominent of peaks can be seen in area of  $2\theta < 10$ . However, the presence of peaks in this area was exhibited that UoB-3 had porous structural. In addition, the pattern of UoB-3 was similar to the simulated pattern reported of IRMOF-74.<sup>[47]</sup> This observation confirmed that the both of structure (UoB-3 & IRMOF-74) were isostructural.

The  $N_2$  adsorption/desorption at 77 K was used to investigate the porosity of synthesized nanostructures. The  $N_2$  sorptometry results showed a typical type IV nitrogen sorption curve according to the IUPAC classification (Figure 1d). This observation indicated that UoB-3 was a mesoporous material. In addition to, the hysteresis loop of curve was type HI that released UoB-3 had narrow distributions of pore size. The analysis of the sorption curve using the Brunauer–Emmett–Teller (BET) method demonstrated that the specific area was approximately  $50 \text{ m}^2 \text{ g}^{-1}$  and the pore volume was  $0.18 \text{ cm}^3 \text{ g}^{-1}$ . Moreover, the mesopore size distribution curve, calculated from Barrett–Joyner–Halenda analysis,

indicated a narrow pore diameter distribution at 16 nm (Figure 1e). The pore size distribution curve confirmed that the surface area of UoB-3 was mainly derived from the mesopore.

In the FT-IR spectrum of UoB-3 nanostructures (Figure 2, a), the corresponding  $\nu(\text{C}=\text{O})$  stretching was observed in the  $1244 \text{ cm}^{-1}$ , whereas  $\nu(\text{OH})$  of the coordinated water molecules was in the  $3450 \text{ cm}^{-1}$ . The band at  $1695 \text{ cm}^{-1}$  established the presence of a coordinated acetate ligand. In addition, the characteristic strong bands of the coordinated carboxylate groups appear at  $1594 \text{ cm}^{-1}$  for the asymmetric stretching and  $1401 \text{ cm}^{-1}$  for the symmetric  $\nu(\text{C}=\text{O})$  one. These values confirmed that  $\text{CO}_2^-$  groups were coordinated to cobalt. The coordination modes of carboxylate to metal could be determined by the values of  $\Delta\nu$  ( $\Delta\nu = \nu_{\text{as}}(\text{COO}) - \nu_{\text{s}}(\text{COO})$ ) for metal carboxylates.<sup>[56]</sup> The observed  $\Delta\nu$  values for UoB-3 indicated a bridging coordination mode for the carboxylate groups; according to these observations, the geometric structure the cobalt was proposed. (Figure 2, b).

According to the obtained data from Elemental CHN and ICP analyses, the molecular formula of UoB-3 nanostructures was suggested as  $\text{Co}_2(\text{bdda})_{1.5}(\text{OAc})_1 \cdot 5\text{H}_2\text{O}$ . The calculated elemental content based on its molecular formula is C (49.91%), N (4.85%), H (3.98%) and Co (15.25%) that appropriately agrees with the real amounts of C (50.43%), N (5.00%), H (3.56%) and Co (13.68%).

The thermal stability of UoB-3 nanostructures was studied by TGA under nitrogen gas over a range of 20–700 °C. The TGA curve indicated two recognizable weight loss steps (Figure 3). The first weight loss (9.69%) from room temperature to 260 °C was attributed to the

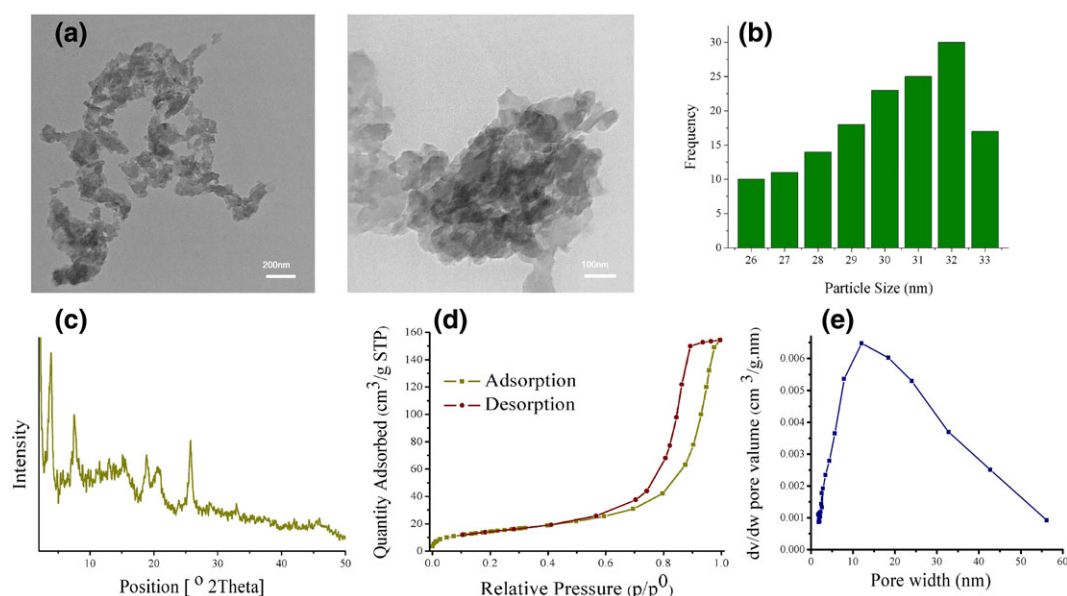


**FIGURE 1** (a) TEM images; (b) Particle size distribution histogram; (c) XRD pattern; (d) Isotherm adsorption–desorption; (e) Pore width of UoB-3

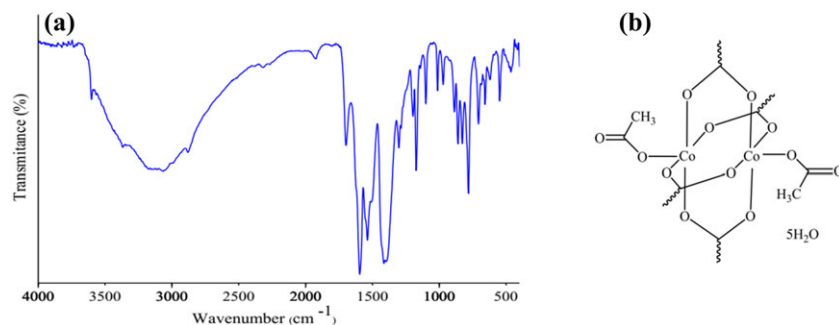


**FIGURE 2** (a) FTIR spectrum of UoB-3; (b) The suggested geometry around of the Co center

loss of water molecules. This observation was in good agreement with the number of water molecules in the proposed molecular formula. Another weight loss (41.77%) in the range of 260–660 °C can be derived from the decomposition of the coordinated organic ligands. Actually, acetate and the part of Schiff base linker decomposed that compatible with the results of CHN and ICP analyses.

### 3.2 | Catalytic studies

UoB-3 nanostructures were exhibited considerable activity for the primary and secondary alcohols oxidation to the corresponding aldehydes or ketones; and Henry reaction between several benzaldehydes and nitromethane in water (Scheme 2).

#### 3.2.1 | Alcohol oxidation

Benzyl alcohol oxidation was chosen as a model substrate in more detail to optimize the reaction variables such as solvent, temperature, the molar ratio of alcohol/oxidant and alcohol/catalyst. Initially, the model reaction was conducted under neat conditions. However, reaction did not proceed in the absence of the catalyst. Therefore,

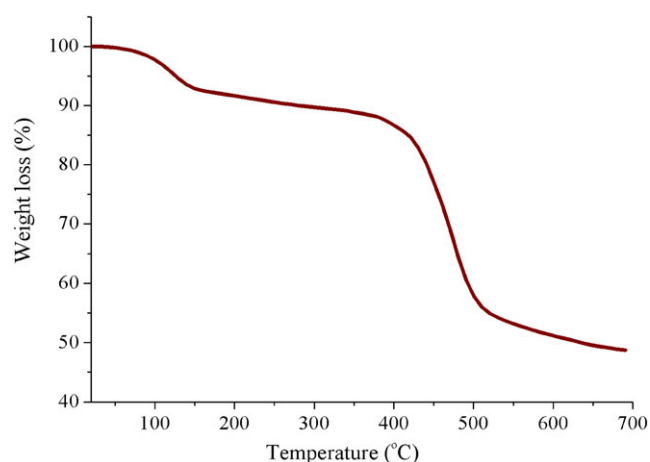
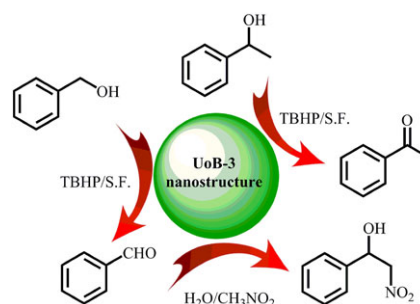


**FIGURE 3** TGA curve of UoB-3 nanostructures

the usage of effective catalyst for the promotion of given reaction was reasonable. In order to the investigation of solvent nature, the model reaction was performed in different solvents and solvent-free conditions (Figure S1). As seen, the best result was given in solvent-free conditions in the presence of UoB-2 as catalyst (Figure S1). It is suggested that open catalytic sites in solvent-free medium is the reason of this observation. After that, the catalytic performance of UoB-3 was evaluated at different temperature (Figure S2). With increasing temperature, the reaction was improved based on yield and rate, gradually. The maximum yield was observed at 65 °C. More increasing in the temperature had no positive effect on the yield and rate of the reaction. Then, the catalyst (Figure S3) and oxidant amount (Figure S4) was optimized. Best yield was obtained in the presence of 2 mol% of UoB-3 and 1.5 mmol of TBHP. The effect of oxidant type was also evaluated with TBHP, NaIO<sub>4</sub>, H<sub>2</sub>O<sub>2</sub> and Oxone under the catalytic influence of UoB-3 in the solvent-free conditions at 65 °C (Figure S5). After the optimization of reaction, the activity of Co (OAc)<sub>2</sub> as the precursor salt of UoB-3 was evaluated, 40% yield was obtained after 60 minutes (Figure S3). Therefore, it can be concluded that the ligand H<sub>2</sub>bdda have an important role in this catalytic system.

With the optimized reaction conditions in hand, we next evaluated the oxidation reaction of primary and secondary alcohols in the presence of UoB-3 nanostructures. The number of available aromatic alcohols bearing electron-donating or electron-withdrawing groups were

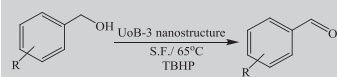


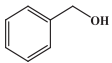
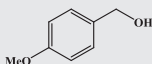
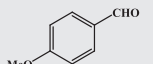
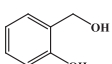
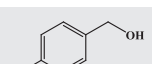
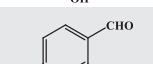
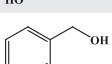
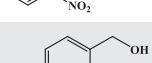
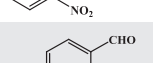
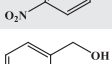
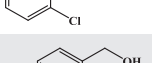
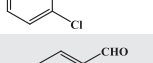
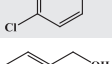
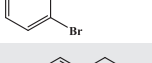
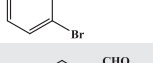
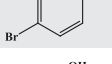
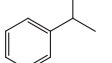
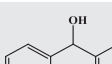
**SCHEME 2** Catalytic activity of UoB-3 in primary/secondary alcohol oxidation and Henry reaction

tested which their results are summarized in Table 1. A slight difference in the yield of the reactions is probably due to the presence of electron-donating/withdrawing functional groups on the benzene ring, which cause the alcohols to be slightly active or inactive.

The mechanism of alcohol oxidation with TBHP in the presence of UoB-3 was investigated. For this reason, the benzyl alcohol oxidation catalyzed by UoB-3 was chosen. PhNH<sub>2</sub> and CBrCl<sub>3</sub> were added to the reaction medium as the oxygen and carbon traps, respectively.

**TABLE 1** Substrate scope for oxidation of primary and secondary benzyl alcohol by UoB-3<sup>a</sup>



Entry	Substrate	Product	Time (min)	Yield (%) <sup>b</sup>
1			60	95
2			45	93
3			60	83
4			60	87
5			75	81
6			75	84
7			45	82
8			45	84
9			60	90
10			60	85
11			90	82
12			90	75
13			90	78

<sup>a</sup>Reaction conditions: Alcohols (1 mmol), TBHP (1.5 mmol), UoB-3 (2 mol%), Solvent free, 65 °C.

<sup>b</sup>Isolated yield.

The reaction yield decreased after adding PhNH<sub>2</sub> or CBrCl<sub>3</sub> from 95% (Table 1, Entry 1) to 2% and 4%, respectively. The results confirmed that the mechanism of alcohol oxidation occurs via the radical mechanism, and it is similar to the proposed mechanism in other cases.<sup>[26,57]</sup> Based on obtained results, it was proposed that the oxidation mechanism may start with the metal-assisted generation of <sup>t</sup>BuOO• (upon reduction of <sup>t</sup>BuOOH by Co (II) center), and continue by the generation of <sup>t</sup>BuO• (upon oxidation of <sup>t</sup>BuOOH by the formed Co (III) center). These radicals act as hydrogen atom abstractors from the alcohols. In the proposed mechanism, the proton transfer steps are the fundamental steps of the above reaction. These steps can be assisted by the linker Schiff base that increase the catalytic activity of UoB-3.

The merit of this operationally catalytic protocol was compared with the previously reported methods (Table 2), in terms of catalyst loading, conversion rate, conversion yield and used conditions in the oxidation of benzyl alcohol as model substrate. Inspection of the results was revealed clearly the superiority of the presented methodology for oxidation of alcohols. Actually, the low amount of used catalyst, the reduced reaction time and the absence of solvent were common advantages of our system.

### 3.2.2 | Henry reaction

The good performance of UoB-3 as heterogeneous catalyst in alcohol oxidation reaction encouraged us to check the catalytic activity of this catalyst in the different reaction. Therefore, the potential catalytic activity of UoB-3 nanostructures was investigated in Henry (or nitroaldol) reaction of nitromethane with various aldehydes. To search for the optimal conditions, benzaldehyde (0.50 mmol) and nitromethane (2.5 mmol) were taken as model substrates with UoB-3 nanostructures as catalyst. The factors that affect reaction including the nature of solvent, amount of catalyst and temperature were screened. Initially, control reactions were examined in the absence of UoB-3 nanostructures but in the presence of Co (OAc)<sub>2</sub> and free linker. No remarkable reaction between benzaldehyde and nitromethane was observed in the absence of nanocatalyst. Actually, the nitroaldol reaction was proceed after an extended reaction time of 24 hours in the presence of Co (OAc)<sub>2</sub> and free linker 18% and 20%, respectively (Figure S7). The model reaction was carried out at 70 °C in different solvents such as water, ethanol, ethyl acetate, acetonitrile and solvent-free condition (Figure S6). Surprisingly, the best result was obtained in water. Thus; water was selected as the sole solvent for further studies. Then, the effect of catalyst

**TABLE 2** Comparison of activities of catalysts towards the alcohol oxidation reaction

Catalyst	Catalyst amount	Conditions	yield	Time (h)	ref
MOF-HPW	50 mg	CTAB/H <sub>2</sub> O <sub>2</sub> /80 °C	98	3	[27]
Fe-MIL-101	1 mol	CH <sub>3</sub> CN/O <sub>2</sub> /75 °C	50	14	[28]
Hf-MOF-808-V	7.5 mol%	Tuloeane/O <sub>2</sub> /105 °C	95	6	[29]
CuPd-MOF	100 mg	Tuloeane/O <sub>2</sub> /130 °C	71	7	[30]
{[Cu(L <sub>1</sub> )-(DMF)]·DMF·H <sub>2</sub> O} <sub>n</sub> <sup>b</sup>	0.2 mol	MW/TBHP/100 °C	81	0.5	[31]
[Co <sub>3</sub> L(PTA) <sub>2.5</sub> (OAc)] <sup>a</sup>	2 mol %	CH <sub>3</sub> CN/TBHP/60 °C	88	24	[32]
MIL-53(Fe)-graphene	15 mg	CCl <sub>4</sub> /visible-light	80	9	[33]
UoB-3	2 mol%	S.F./TBHP/65 °C	95	1	This work

<sup>a</sup>PTA: *p*-phthalic acid.

<sup>b</sup>L:5-{(pyridin-4-ylmethyl)amino} isophthalic acid.

amount was studied. An increase of the catalyst amount from 1.0 to 3.0 mol% was enhanced the reaction yield from 18% to 83%, respectively; but a further rise of that amount was not improved the product yield (Figure S7). Afterwards, the investigation of the temperature effect was revealed that varying the temperature from room temperature to 70 °C improved the yield of  $\beta$ -nitroalkanol from 20 to 83%, however, a further temperature increase had not the positive effect (Figure S8).

With having the optimized conditions of reaction, the catalytic activity of UoB-3 was examined the reaction of different substituted aromatic aldehydes with nitromethane, producing the corresponding  $\beta$ -nitroalkanols with yields from 62 to 88%. The results revealed that aryl aldehydes bearing an electron-withdrawing group were exhibited higher reactivity (Table 3, entries 2 and 7) as compared to those having electron-donating moieties (Table 3, entries 5 and 10). It may be related to an increase of the electrophilicity of the substrate in the former case.

Furthermore, the catalytic activity of UoB-3 was extended to the reaction of benzaldehyde and nitroalkanes with various molecular size including nitromethane (2.0 Å × 3.3 Å), nitroethane (2.2 Å × 3.9 Å) and nitropropane (2.2 Å × 5.6 Å)]. The obtained results released that the yield of reaction was systematically depended on the molecular size of nitroalkanes (Table 4). Actually, the reaction yield decreased as the molecular size of nitroalkanes increased. These observations can help to get a comprehensive the reaction mechanism and reaction center. Based on the selective-size behavior of UoB-3, it can be concluded that the reaction catalyst in the interior sites and not only by the exterior ones.

The reaction mechanism for the Henry reaction catalyzed by UoB-3 should be similar to the reported cases with the related catalytic systems.<sup>[58,59]</sup> For giving a

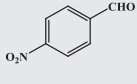
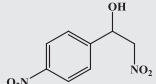
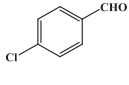
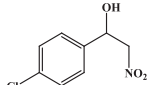
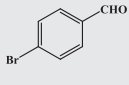
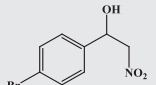
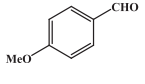
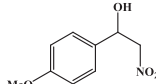
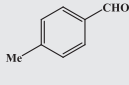
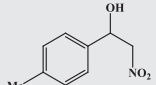
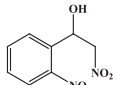
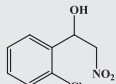
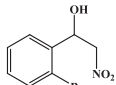
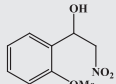
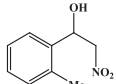
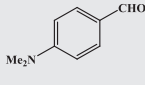
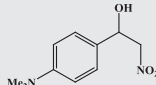
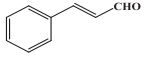
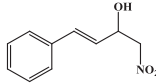
nitronate species, the linker assisted the deprotonation of the methylene group of nitromethane. Then, benzaldehyde was activated by metal center towards its electrophilic attack. Finally, the formation of C – C bond upon nucleophilic was performed by addition of the nitronate to the carbonyl group of aldehyde to give the  $\beta$ -nitroalkanol. The abstraction of proton from nitroalkane and the protonation of the C – C coupled species can be assisted by the linker (with an azomethine group) and by water (amphoteric behavior), thus this probably accounts for the good activity of our catalysts in the presence of water Scheme 3.

The catalytic efficiency of UoB-3 nanostructures in comparison with various MOFs that had catalyzed Henry reaction was presented in Table 5. UoB-3 nanostructures had the advantages of being rather cheap and easy-to-prepare. Moreover, organic solvents have been utilized in the some of the reported cases for the Henry reaction, and there were only very few examples where water has been applied. In this work, interestingly, the best results were obtained in aqueous medium compared with the organic solvents. Using of water as solvent had many advantages such as non-toxic, safe, and environmentally benign.

### 3.2.3 | Recyclability and heterogeneity tests

The recyclability and the heterogeneous nature of UoB-3 nanostructures were investigated in the both of alcohol oxidation and Henry reactions. The nanostructures were recovered from the reaction mixture after appropriate time for the next reaction run by centrifugation, washing with ethanol, and then drying in the oven. As shown in Figure 4 (right), the significant changes were not observed in the activity of UoB-3 after five runs. FT-IR

**TABLE 3** Henry reaction of various aldehydes and nitromethane with UoB-3<sup>a</sup>

Entry	Substrate	Product	Yield (%) <sup>b</sup>
1			83
2			88
3			85
4			83
5			78
6			74
7			78
8			75
9			72
10			65
11			62
12			68
13			80

<sup>a</sup>Condition reaction: Benzaldehyde (1 mmol), Nitromethane (5 mmol), UoB-3 (3 mol%), H<sub>2</sub>O (1 ml), 70 °C, 24 hr;

<sup>b</sup>Isolated yield.

spectra of reused UoB-3 compared with its fresh were revealed that the internal structure of it was maintained intact even after the five cycles of the reaction (Figure S9).

The hot filtration test was carried out for Henry reaction in order to clarify if the catalytic process was heterogeneous or homogeneous. For this purpose, a controlled experiment with UoB-3 was performed until an intermediate yield (ca. 45%) was observed (12 hr). Then, the catalyst was removed, kept the catalyst free reaction solution under the same conditions and was stirred for additional 36 hrs. The results indicated that the yield of  $\beta$ -nitroalkanol did not increase appreciably after removal of the solid catalyst (Figure 4, left). Additionally, the amount of cobalt was determined in the filtrated solution, after the separation of the catalyst, was only 0.01% of the amount used in the reaction thus ruling out any significant leaching of the catalyst. These observations demonstrated that the catalysis was heterogeneous in nature.

### 3.3 | Antibacterial activity

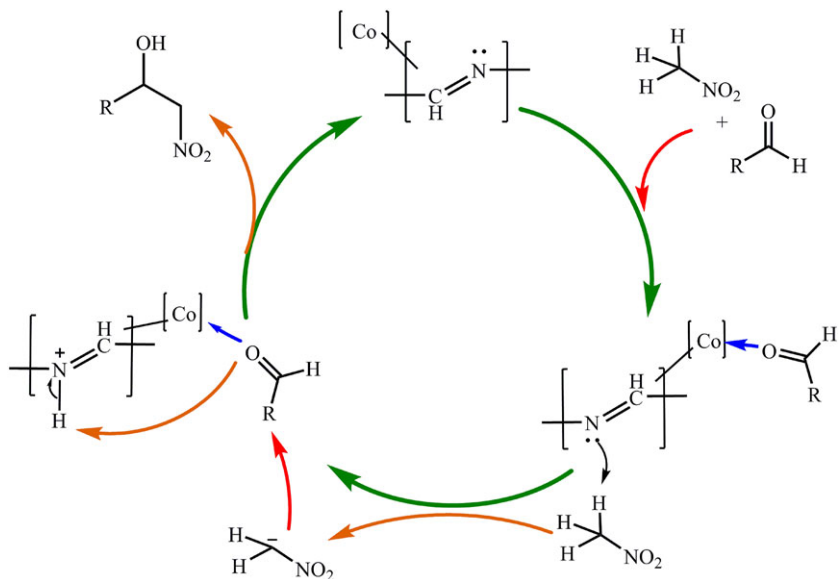
The advantages of MOFs as new, highly functional compounds with biological activity might come from their composition, structure, and very high internal volume. In addition to, the benefits to using MOFs over natural and synthetic polymers is their uniformity of the speciation and distribution of metal active sites. As regards, medicinal applications of MOFs might be limited because of their low solubility.<sup>[60]</sup> Accordingly, the developing novel MOFs with therapeutic activity is very important. Therefore, the antibacterial activity of UoB-3 nanostructures was evaluated in this work. Gram-negative bacteria, *Escherichia coli* and Gram-positive bacteria, *Bacillus cereus* were chosen as model microorganisms at the concentration of 80  $\mu$ l by the Agar well diffusion method. The both of the bacteria are commonly found in water. The standard zone of inhibition test, a qualitative test

**TABLE 4** Henry reaction of benzaldehydes and various nitroalkanes with UoB-3<sup>a</sup>

Entry	Substrate	Nitroalkane	Yield (%) <sup>b</sup>
1		CH <sub>3</sub> NO <sub>2</sub>	83
2			71
3			46

<sup>a</sup>Condition reaction: Benzaldehyde (1 mmol), Nitroalkane (5 mmol), UoB-3 (3 mol%), H<sub>2</sub>O (1 ml), 70 °C, 24 h;

<sup>b</sup>Isolated yield.



**SCHEME 3** Proposed catalytic cycle for the Henry reaction catalyzed by UoB-3

**TABLE 5** Comparison of activities of catalysts towards the Henry reaction using aldehyde and nitromethane

Catalyst	Aldehyde	solvent/temp/time	yield	ref
Cu(L)(H <sub>2</sub> O) <sub>4</sub> (L = 2-propionamidoterephthalate)	Benzaldehyde	H <sub>2</sub> O/70 °C/30 h	71	[49]
[Cu <sub>3</sub> (pdtc)L <sub>2</sub> (H <sub>2</sub> O) <sub>3</sub> ].2DMF.10H <sub>2</sub> O (HL: 4-(2-(pyridin-4-yl)vinyl) benzoic acid)	Benzaldehyde	1,4-dioxane/70 °C/36 h	50	[61]
NH <sub>2</sub> -Tb-MOF	Benzaldehyde	EtOAc/90 °C/24 h	87	[50]
[Cu(L)-(DMF)] · DMF · H <sub>2</sub> O (H <sub>2</sub> L: 5-((Pyridin-4-ylmethyl)amino) isophthalic acid)	Benzaldehyde	H <sub>2</sub> O/75 °C/40 h	84	[31]
[Cd(L)] <sub>n</sub> (H <sub>2</sub> L: 5-((Pyridin-4-ylmethyl)amino)isophthalic acid)	Benzaldehyde	H <sub>2</sub> O/75 °C/40 h	69	[31]
[[Cd <sub>2</sub> (L-glu) <sub>2</sub> (bpe) <sub>3</sub> (H <sub>2</sub> O)] · 2H <sub>2</sub> O]	Benzaldehyde	MeOH/R.T./72 h	89	[48]
[Cu <sub>4</sub> (HL) <sub>2</sub> (H <sub>2</sub> O) <sub>4</sub> (MeO) <sub>4</sub> ] <sub>n</sub> (H <sub>3</sub> L: (2S,2'S,2''S)-2,2',2''-benzenetricarbonyltris (azanediyl)) tripropanoic acid)	Benzaldehyde	MeOH/70 °C/24 h	89	[59]
UoB-3	Benzaldehyde	H <sub>2</sub> O/70 °C/24 h	83	This work

performed under static conditions, was used for investigation of anti-bacterial activity. Its results for individual bacterial culture was shown in Figure 5. The bacterial growth below the contact area between the *E. coli*/*B.*

*cereus* and the UoB-3 was highly inhibited. The diameter of inhibition zones (cm) around UoB-3 nanostructures were for *E. coli* and *B. cereus*  $2.3 \pm 1$  and  $3.5 \pm 1$ , respectively. The differences in the diameter of zone of

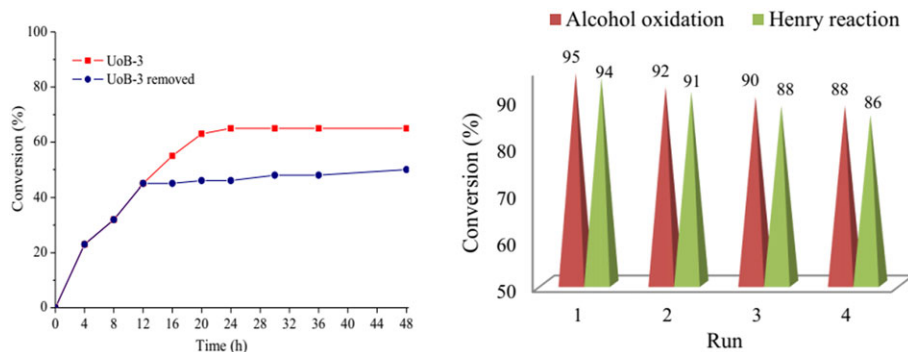


**FIGURE 4** (left) The hot leaching test for Henry reaction based on UoB-3 nanostructures; (right) Catalyst recycling test for alcohol oxidation and Henry reaction.



**FIGURE 5** Inhibition areas for UoB-3 nanostructures (a) *B. Cereus*, (b) *E. Coli*

inhibition for *E. coli*/*B. cereus* might be due to the difference in the susceptibility of different bacteria to UoB-3. The difference in cell structure, physiology and metabolism of Gram-positive and Gram-negative bacteria might be effect on their sensitivity toward UoB-3 nanostructures. However, the present study clearly was exhibited that UoB-3 nanostructures indicated good activity against both Gram-negative and positive organism.

#### 4 | CONCLUSION

In conclusion, the Co-MOF nanostructures were synthesized *via* a simple and fast methods at room temperature by using the Schiff base linker, 4,4'-[benzene-1,4-diylbis (methylidenenitrilo)] dibenzoic acid ( $H_2bda$ ). As a heterogeneous catalyst, these nanostructures were exhibited an excellent catalytic performance in the oxidation of primary/secondary alcohols. As well as, UoB-3 was catalyzed the Henry reaction of nitromethane with various aldehydes in aqueous medium producing the corresponding  $\beta$ -nitroalknols in high yields. The preferential use of water instead of an organic solvent was a significant feature towards green catalysis for the preparation because water was safe, economical, environmentally benign, and nontoxic. In addition, UoB-3 was highly stable and, could be recycled and reused a number of times without loss of catalytic performance in the both reactions. More importantly, the investigation of antibacterial properties of UoB-3 indicated that they were exhibited a strong antibacterial activity against microorganism growth.

#### ACKNOWLEDGEMENTS

This work was supported by Iran National Science Foundation (Project No. 96008530). We also thank University of Birjand Research Council.

#### ORCID

Sima Aryanejad  <https://orcid.org/0000-0002-5145-3734>  
Ghodsieh Bagherzade  <https://orcid.org/0000-0002-7417-2214>

#### REFERENCES

- [1] J. H. Clark, *Green Chem.* **1999**, *1*, 1.
- [2] P. Anastas, N. Eghbali, *Chem. Soc. Rev.* **2010**, *39*, 301.
- [3] A. Maleki, M. Aghaei, N. Ghamari, *Appl. Organomet. Chem.* **2016**, *30*, 939.
- [4] A. Maleki, H. Movahed, R. Paydar, *RSC Adv.* **2016**, *6*, 13657.
- [5] A. Maleki, P. Ravaghi, M. Aghaei, H. Movahed, *Res. Chem. Intermed.* **2017**, *43*, 5485.
- [6] A. Maleki, E. Akhlaghi, R. Paydar, *Appl. Organomet. Chem.* **2016**, *30*, 382.
- [7] A. Maleki, R. Firouzi-Haji, Z. Hajizadeh, *Int. J. Biol. Macromol.* **2018**, *116*, 320.
- [8] A. Maleki, P. Zand, Z. Mohseni, R. Firouzi-Haji, *Nano-Structures & Nano-Objects* **2018**, *16*, 31.
- [9] K. K. Gangu, S. Maddila, S. B. Mukkamala, S. B. Jonnalagadda, *Inorganica Chim. Acta* **2016**, *446*, 61.
- [10] H. Furukawa, K. E. Cordova, M. O'Keefe, O. M. Yaghi, *Science* **2013**, *341*, 1230444.
- [11] N. Stock, S. Biswas, *Chem. Rev.* **2011**, *112*, 933.
- [12] X. Yang, Q. Xu, *Cryst. Growth Des.* **2017**, *17*, 1450.
- [13] W. Zhou, Y.-P. Wu, J. Zhao, W.-W. Dong, X.-Q. Qiao, D.-F. Hou, X. Bu, D.-S. Li, *Inorg. Chem.* **2017**, *56*, 14111.
- [14] A. Ibrahim, Y. S. Lin, *Ind. Eng. Chem. Res.* **2016**, *55*, 8652.
- [15] L. Zhu, X.-Q. Liu, S. L.-B. Jiang, *Chem. Rev.* **2017**, *117*, 8129.
- [16] J. Liu, L. Chen, H. Cui, J. Zhang, L. Zhang, C.-Y. Su, *Chem. Soc. Rev.* **2014**, *43*, 6011.
- [17] X. Chen, R. Tong, Z. Shi, B. Yang, H. Liu, S. Ding, X. Wang, Q. Lei, J. Wu, W. Fang, *ACS Appl. Mater. Interfaces* **2018**, *10*, 2328.
- [18] P. Horcajada, R. Gref, T. Baati, P. K. Allan, G. Maurin, P. Couvreur, G. Férey, R. E. Morris, C. Serre, *Chem. Rev.* **2011**, *112*, 1232.
- [19] A. Herbst, A. Khutia, C. Janiak, *Inorg. Chem.* **2014**, *53*, 7319.

- [20] A. Foucault-Collet, K. A. Gogick, K. A. White, S. Villette, A. Pallier, G. Collet, C. Kieda, T. Li, S. J. Geib, N. L. Rosi, *Proc. Natl. Acad. Sci.* **2013**, *110*, 17199.
- [21] R. Ciriminna, V. Pandarus, F. Béland, Y.-J. Xu, M. Pagliaro, *Org. Process Res. Dev.* **2015**, *19*, 1554.
- [22] M. N. Kopylovich, A. P. C. Ribeiro, E. C. B. A. Alegria, N. M. R. Martins, L. M. Martins, A. J. L. Pombeiro, *Advances in Organometallic Chemistry*, Elsevier, New York **2015**, 91.
- [23] A. Maleki, *Ultrason. Sonochem.* **2018**, *40*, 460.
- [24] A. Maleki, T. Kari, *Catal. Letters* **2018**, *148*, 2929.
- [25] G. B. Shul'pin, M. V. Kirillova, L. S. Shul'pina, A. J. L. Pombeiro, E. E. Karslyan, Y. N. Kozlov, *Catal. Commun.* **2013**, *31*, 32.
- [26] D. Shen, C. Miao, D. Xu, C. Xia, W. Sun, *Org. Lett.* **2014**, *17*, 54.
- [27] J. Zhu, M. Shen, X. Zhao, P. Wang, M. Lu, *Chempluschem* **2014**, *79*, 872.
- [28] Z. Jin, Y. Luan, M. Yang, J. Tang, J. Wang, H. Gao, Y. Lu, G. Wang, *RSC Adv.* **2015**, *5*, 78962.
- [29] K. Otake, Y. Cui, C. T. Buru, Z. Li, J. T. Hupp, O. K. Farha, *J. Am. Chem. Soc.* **2018**, *140*, 8652.
- [30] P. Guo, C. Froese, Q. Fu, Y.-T. Chen, B. Peng, W. Kleist, R. A. Fischer, M. Muhler, Y. Wang, *J. Phys. Chem. C* **2018**, *122*, 21433.
- [31] A. Karmakar, L. M. Martins, S. Hazra, M. F. C. Guedes da Silva, A. J. L. Pombeiro, *Cryst. Growth Des.* **2016**, *16*, 1837.
- [32] J.-C. Wang, F.-W. Ding, J.-P. Ma, Q.-K. Liu, J.-Y. Cheng, Y.-B. Dong, *Inorg. Chem.* **2015**, *54*, 10865.
- [33] Z. Yang, X. Xu, X. Liang, C. Lei, Y. Wei, P. He, B. Lv, H. Ma, Z. Lei, *Appl. Catal. B Environ.* **2016**, *198*, 112.
- [34] M. Shibasaki, M. Kanai, S. Matsunaga, N. Kumagai, *Bifunctional Molecular Catalysis*, Springer, Berlin **2011**.
- [35] J. Otevreil, P. Bobal, *J. Org. Chem.* **2017**, *82*, 8342.
- [36] M. H. Abdellattif, M. Mokhtar, *Catalysts* **2018**, *8*, 133.
- [37] A. G. Doyle, E. N. Jacobsen, *Chem. Rev.* **2007**, *107*, 5713.
- [38] J.-M. Lee, J. Kim, Y. Shin, C.-E. Yeom, J. E. Lee, T. Hyeon, B. M. Kim, *Tetrahedron: Asymmetry* **2010**, *21*, 285.
- [39] I. V. Kutovaya, O. I. Shmatova, V. G. Nenajdenko, *Mendeleev Commun.* **2018**, *28*, 81.
- [40] M. Yamaguchi, Y. Igarashi, R. S. Reddy, T. Shiraishi, M. Hirama, *Tetrahedron* **1997**, *53*, 11223.
- [41] M. N. Kopylovich, A. Mizar, M. F. C. Guedes da Silva, T. C. O. Mac Leod, K. T. Mahmudov, A. J. L. Pombeiro, *Chem. – Eur. J.* **2013**, *19*, 588.
- [42] D. Qin, W. Lai, D. Hu, Z. Chen, A. Wu, Y. Ruan, Z. Zhou, H. Chen, *Chem. – Eur. J.* **2012**, *18*, 10515.
- [43] E. Wolińska, *Tetrahedron* **2013**, *69*, 7269.
- [44] B. Ni, J. He, *Tetrahedron Lett.* **2013**, *54*, 462.
- [45] R. Maggi, D. Lanari, C. Oro, G. Sartori, L. Vaccaro, *European J. Org. Chem.* **2011**, *2011*, 5551.
- [46] N. Neelakandeswari, G. Sangami, P. Emayavaramban, R. Karvembu, N. Dharmaraj, H. Y. Kim, *Tetrahedron Lett.* **2012**, *53*, 2980.
- [47] M. Sutradhar, M. F. C. G. da Silva, A. J. L. Pombeiro, *Catal. Commun.* **2014**, *57*, 103.
- [48] B. Ugale, S. S. Dhankhar, C. M. Nagaraja, *Inorg. Chem. Front.* **2017**, *4*, 348.
- [49] L.-X. Shi, C.-D. Wu, *Chem. Commun.* **2011**, *47*, 2928.
- [50] J. Huang, C. Li, L. Tao, H. Zhu, G. Hu, *J. Mol. Struct.* **2017**, *1146*, 853.
- [51] N. M. R. Martins, K. T. Mahmudov, M. F. C. G. da Silva, L. M. Martins, F. I. Guseinov, A. J. L. Pombeiro, *Catal. Commun.* **2016**, *87*, 49.
- [52] A. Tabacaru, N. Khaferaj, L. M. Martins, E. C. B. A. Alegria, R. S. Chay, C. Giacobbe, K. V. Domasevitch, A. J. L. Pombeiro, S. Galli, C. Pettinari, *Inorg. Chem.* **2016**, *55*, 5804.
- [53] J. Mlynarski, S. Baś, *Chem. Soc. Rev.* **2014**, *43*, 577.
- [54] S. Aryanejad, G. Bagherzade, A. Farrokhi, *Appl. Organomet. Chem.* **2018**, *32*, e3995.
- [55] S. Aryanejad, G. Bagherzade, A. Farrokhi, *Inorg. Chem. Commun.* **2017**, *81*, 37.
- [56] K. Nakamoto, K. Nakamoto, *Infrared and Raman Spectra of Inorganic and Coordination Compounds*, Wiley, New York **1977**.
- [57] M. Sutradhar, L. M. Martins, M. F. C. G. da Silva, A. J. L. Pombeiro, *Appl. Catal. A Gen.* **2015**, *493*, 50.
- [58] S. Hazra, A. Karmakar, C. Maria de Fátima, R. Boča, A. J. L. Pombeiro, *New J. Chem.* **2015**, *39*, 3424.
- [59] A. Karmakar, C. L. Oliver, S. Roy, L. Öhrström, *Dalt. Trans.* **2015**, *44*, 10156.
- [60] G. Wyszogrodzka, B. Marszałek, B. Gil, P. Doroczyński, *Drug Discovery Today* **2016**, *21*, 1009.
- [61] A. Karmakar, S. Hazra, M. F. C. G. da Silva, A. J. L. Pombeiro, *New J. Chem.* **2014**, *38*, 4837.

## SUPPORTING INFORMATION

Additional supporting information may be found online in the Supporting Information section at the end of the article.

**How to cite this article:** Aryanejad S, Bagherzade G, Moudi M. Design and development of novel Co-MOF nanostructures as an excellent catalyst for alcohol oxidation and Henry reaction, with a potential antibacterial activity. *Appl Organometal Chem.* 2019;e4820. <https://doi.org/10.1002/aoc.4820>